NOAA Technical Report NESDIS 27

Estimation of Broadband Planetary Albedo from Operational Narrowband Satellite Measurements

Washington, D.C.
April 1987

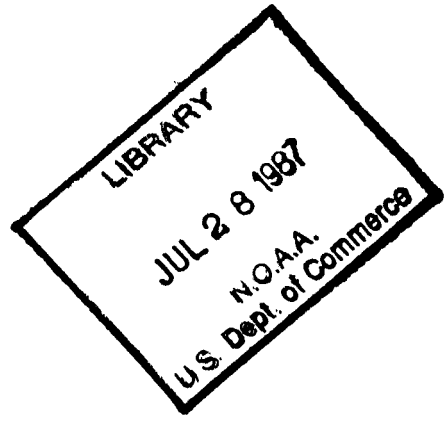

U.S. DEPARTMENT OF COMMERCE
National Oceanic and Atmospheric Administration
National Environmental Satellite, Data, and Information Service

NOAA TECHNICAL REPORTS

National Environmental Satellite, Data, and Information Service

The National Environmental Satellite, Data, and Information Service (NESDIS) manages the Nation's civil operational Earth-observing satellite systems, as well as global national data bases for meteorology, oceanography, geophysics, and solar-terrestrial sciences. From these sources, it develops and disseminates environmental data and information products critical to the protection of life and property, national defense, the national economy, energy development and distribution, global food supplies, and the development of natural resources.

Publication in the NOAA Technical Report series does not preclude later publication in scientific journals in expanded or modified form. The NESDIS series of NOAA Technical Reports is a continuation of the former NESS and EDIS series of NOAA Technical Reports and the NESC and EDS series of Environmental Science Services Administration (ESSA) Technical Reports.

These reports are available from the National Technical Information Service (NTIS), U.S. Department of Commerce, Sills Bldg., 5285 Port Royal Road, Springfield, VA 22161. Prices on request for paper copies or microfiche.

A more complete listing of these reports, by title and NTIS accession number, is available from the Assessment and Information Services Center, National Oceanic and Atmospheric Administration, Code E/AI13, Page Bldg. 2, 3300 Whitehaven Street, N.W., Washington, DC 20235. A partial listing of more recent reports appears below:

NESS Series

NESS 89 A Statistical Approach to Rainfall Estimation Using Satellite and Conventional Data. Linwood F. Whitney, Jr. April 1982. (PB82 215435)

NESS 90 Total Precipitable Water and Rainfall Determinations From the SEASAT Scanning Multichannel Microwave Radiometer (SMMR). John C. Alishouse, May 1982. (PB83 138263)

NESS 91 Numerical Smoothing and Differentiation by Finite Differences. Henry E. Fleming and Lawrence J. Crone, May 1982. (PB82-258385)

NESS 92 Satellite Infrared Observations of Oceanic Long Waves in the Eastern Equatorial Pacific 1975 to 1981. Richard Legeckis, November 1982. (PB83 161133)

NESS 93 A Method for Improving the Estimation of Conditional Instability from Satellite Retrievals. W.E. Togstad, J.M. Lewis, and H.M. Woolf, November 1982. (PB83 169938)

EDIS Series

EDS 29 GATE Convection Subprogram Data Center: Final Report on Rawinsonde Data Validation. Robert W. Reeves, March 1978. (PB-281-861)

EDS 30 Gamma Distribution Bias and Confidence Limits. Harold L. Crutcher and Raymond L. Joiner, September 1978. (PB-289-721)

EDIS 31 Calibration and Intercomparison of the GATE C-Band Radars. M. Hudlow, R. Arkell, V. Patterson, P. Pytlowany, F. Richards, and S. Geotis (MIT), November 1979. (PB81 120305)

EDIS 32 Distribution of Radiosonde Errors. Harold L. Crutcher, May 1979. (PB-297-383)

EDIS 33 Accurate Least-Squares Techniques Using the Orthogonal Function Approach. Jerry Sullivan, March 1980. (PB80 223241)

EDIS 34 An Application of Stochastic Forecasting to Monthly Averaged 700 mb Heights. Albert Koscielny, June 1982. (PB82 244625)

NESDIS Series

NESDIS 1 Satellite Observations on Variations in Southern Hemisphere Snow Cover. Kenneth F. Dewey and Richard Heim, Jr., June 1983. (PB83 252908)

NESDIS 2 NODC 1 An Environmental Guide to Ocean Thermal Energy Conversion (OTEC) Operations in the Gulf of Mexico. National Oceanographic Data Center (DOC/NOAA Interagency Agreement Number EX-76-A-29-1041), June 1983. (PB84 115146)

NESDIS 3 Determination of the Planetary Radiation Budget From TIROS-N Satellites. Arnold Gruber, Irwin Ruff, and Charles Earnest, August 1983. (PB84 100916)

NESDIS 4 Some Applications of Satellite Radiation Observations to Climate Studies. T. S. Chen, George Ohring, and Haim Ganot, September 1983. (PB84 108109)

NESDIS 5 A Statistical Technique for Forecasting Severe Weather From Vertical Soundings by Satellite and Radiosonde. David L. Keller and William L. Smith, June 1983. (PB84 114099)

(Continued on inside back cover)

NOAA Technical Report NESDIS 27

Estimation of Broadband Planetary Albedo from Operational Narrowband Satellite Measurements

James E. Wydick
NOAA/Satellite Research Laboratory
Washington, D.C. 20233

Paul A. Davis
Research and Data Systems, Inc.
Lanham, Md.

Arnold Gruber
NOAA/Satellite Research Laboratory
Washington, D.C. 20233

April 1987

U.S. DEPARTMENT OF COMMERCE
Malcolm Baldridge, Secretary

National Oceanic and Atmospheric Administration
Anthony J. Calio, Under Secretary

National Environmental Satellite, Data, and Information Service
Thomas N. Pyke, Jr., Assistant Administrator

National Oceanic and Atmospheric Administration
TIROS Satellites and Satellite Meteorology

ERRATA NOTICE

One or more conditions of the original document may affect the quality of the image, such as:

Discolored pages
Faded or light ink
Binding intrudes into the text

This has been a co-operative project between the NOAA Central Library and the Climate Database Modernization Program, National Climate Data Center (NCDC). To view the original document contact the NOAA Central Library in Silver Spring, MD at (301) 713-2607 x124 or Library.Reference@noaa.gov.

HOV Services
Imaging Contractor
12200 Kiln Court
Beltsville, MD 20704-1387
January 26, 2009

I/11571

CONTENTS

TABLES

FIGURES

Blank page retained for pagination

ESTIMATION OF BROADBAND PLANETARY ALBEDO FROM OPERATIONAL NARROWBAND SATELLITE MEASUREMENTS

Abstract

This study presents a scene independent algorithm for estimating broadband planetary (top-of-atmosphere) albedo using NOAA/AVHRR narrowband satellite data. Initial results from a radiative transfer model investigation are given, followed by empirical coefficients which were deduced through multivariant regression analysis of Nimbus-7/ERB braodband data and/NOAA-7/AVHRR narrowband data. Planetary scenes were grouped into five major categories. Strong variations in the two channel AVHRR narrowband albedo observations were noted for different scene classifications which emphasize the potential error in using a single AVHRR channel 1 (0.58-0.68 um) albedo determination as has historically been done. We found that while individual scene regressions have significantly different regression characteristics; they allow a single regression when all surfaces are taken together due to their natural albedo range. We present scene independent coefficients relating AVHRR narrowband channels 1 and 2 to ERB broadband with an explained

variance of 0.956. Individual scene analyses are also presented but the emphasis of this work was the scene independent studies. The results presented should allow improved albedo calculations when one is limited to AVHRR narrowband data.

ESTIMATION OF BROADBAND PLANETARY ALBEDO FROM OPERATIONAL NARROWBAND SATELLITE MEASUREMENTS

I. INTRODUCTION

Operational satellite platforms provide global data from multispectral narrowband radiometric scanners (e.g., the AVHRR) with small fields of view. With proper adjustments these data can be used to determine estimates of the distribution of the earth's radiation budget components. Typically, most narrowband shortwave measurements have emphasized the visible spectral range, say between 0.55 and 0.75 um. Aside from measurement calibration, the conversion of the shortwave narrowband data into the average planetary albedo requires adjustments to account for

1) Spectral expansion from filtered narrowband to unfiltered broadband radiance over the shortwave spectrum from about 0.24 to 4.2 um;

2) Integration over all possible exitant angles for a given illumination direction, and

3) Integration over all pertinent solar zenith angles to

account for all illumination and sky conditions during a given day.

These adjustments are dependent on the type of underlying background (water, land, clouds, snow) and are indirectly impacted by the actual space and time scale selected for data summary. Only the first of these adjustments constituted the principal goal of this work.

Earlier radiation budget estimates (Gruber and Winston, 1978) simply converted the narrowband radiance measurement (regardless of background) into an isotropic albedo, for which the emergent radiance is considered the same in all directions, and further assumed that the isotropic albedo inferred from the narrowband was identical to that from the broadband. Additionally, the albedo for the time of satellite passage was considered representative of that for the entire day. Subsequent studies, based primarily on results obtained in conjuction with ERB measurements from the Nimbus-7 satellite, have addressed all of the adjustments mentioned above. This study seeks to derive an empirical narrowband to broadband relationships for AVHRR channels 1 and 2, while retaining the assumption of isotropy.

1.1 Background Scene

The shortwave radiance emanating from the top of the atmosphere (TOA) is determined by the variable properties of the underlying surface, by atmospheric molecular/aerosol absorption and scattering, and especially by clouds. If the surface reflectance is low, as for the ocean outside of the specular angle or the lowest sun elevation angles, then atmospheric scattering will dominate the TOA albedo. For other surfaces or clouds, atmosheric scattering plays a secondary role. The general background types could be ranked according to increasing TOA shortwave radiance or albedo: ocean, vegetated land, desert, cloud, and icecap snow. Although there is some overlap between desert and cloud reflectances, or between cloud and snow, the magnitudes themselves generally distinguish different types--with the exception of specular reflection from water. Thus, for the purpose of relating narrowband and broadband radiances in a general way, it may not be necessary to make the relationship scene dependent; instead, data from all scene types may be combined. (Scene identification may still be necessary for angular adjustments of the broadband radiance.) In any case, depending on scale, explicit scene identification is not always possible since a mixture of types is not uncommon. The practicality of a unique linear definition for the narrowband-broadband relationship for a specific surface type may be questionable. For example,

non-specular shortwave data from over a clear ocean may lead to a single cluster of measurements with no obvious statistical relationship. Here the variations of the narrowband-broadband points would have to be described through a detailed physical model with other input information.

1.2 Spectral Range

The translation of a filtered narrowband radiance measurement to the unfiltered broadband radiance depends on the spectral nature of the narrowband filter. Presumably, the spectral ranges of the narrowband filter will sample characteristic absorption/scattering regions of the atmosphere and cover representative background surfaces. The greater the spectral range or number of narrowband spectral intervals (especially the independent ones), the greater will be the information content on the broadband radiances.

Spectral variations of the albedo over various background surfaces are known from specific empirical data (Bowker, et al., 1985) and from various theoretical computations (e.g., Wiscombe and Warren, 1980; Briegleb and Ramanathan, 1982). Algorithms relating radiances from particular narrow spectral intevals to the broadband shortwave radiance have been developed previously (Wydick and Davis, 1983; Minnis and Harrison 1984; Davis, et al., 1984) and are under current development.

1.3 Viewing and Illumination

In accomplishing the spectral expansion from narrowband to broadband it is assumed that comparisons of narrowband and broadband data are based on the same viewing and illumination conditions. In fact, such an empirically derved relationship is valid only for matching angular conditions. Application of the broadband shortwave radiance derived from the relationship, therefore, would still require integration over the entire hemispheric solid angle of view (to obtain instantaneous shortwave flux density or albedo) and over all solar zenith angles encountered during the day (to obtain daily average albedo). It is possible to generate angular models, perform these integrations, and store results in tables in the form of factors to be applied to the instantaneous isotropic albedos derived from the broadband-narrowband relationship presented here. However, use of the tabulated factors to define products such as the daily average albedo requires more information than broadband radiance or isotropic albedo. In particular, some information on the general surface type is required. Furthermore, selection of the appropriate anisotropic integration factor requires the solar zenith, satellite zenith, and relative azimuth angles. For the daily average albedo correction factor, the solar time and the latitude of the viewed point must be known. Tabulated data suitable for the angular adjustments have

been derived from Nimbus-7 ERB data and are discussed by Jacobowitz et al., 1984 and Stowe and Fromm, 1984.

An alternative approach to the estimation of the broadband shortwave parameters from narrowband measurements is first to estimate the narrowband albedo, for which a narrowband bidirectional model is required, then to relate the instantaneous narrowband albedo with the instantaneous broadband albedo.

2.0 DEFINITIONS

In order to establish a basis for evaluating the merit of a narrowband-broadband shortwave relationship, it is first necessary to define the objective of the desired relationship. Once an objective is established then an acceptable procedure is devised for developing an appropriate relationship, even if the derived relationship may not be suitable for any other purpose.

Our major goal is to define a relationship that will make it feasible to use narrowband radiance measurements in the specification of the global distribution of radiation budget parameters (on the scales of days and 500 km). Furthermore, the objective of the application is to employ the conversion from narrowband to broadband on a routine real-time operational basis. Such a robust relationship could be anticipated to be insensitive to fine detail. With the relationship a narrowband radiance (for any angle) would be converted into a broadband

radiance (for the same angle). Given the broadband radiance, a user could then employ established bidirectional models (to convert to broadband flux density and albedo) and directional models (to convert from instantaneous to daily average albedo).

A definition of the desired product requires first a definition of pertinent terms and parameters:

A = daily average albedo

L = spectral radiance from earth-atmosphere

S = solar spectral irradiance

δ = solar zenith angle

θ = satellite zenith angle

ϕ = relative azimuth angle

H = sunlit half-day, the time between sunset or sunrise and noon

$\omega_{\lambda(i)}$ = spectral response of filter for ith interval

L_i = filtered radiance for ith spectral interval

$$= \int_0^\infty L_\lambda \omega_{\lambda(i)} d\lambda$$

I_i = filtered normal solar irradianced in ith spectral interval

$$= \int_0^\infty S_\lambda \omega_\lambda(i)\, d\lambda$$

$E_i = \pi L_i / I_i$, the scaled radiance, or normal-sun isotropic albedo, for ith narrowband

$\rho_i = L_i / (I_i \cos\zeta)$, the bidirectional reflectance

$\alpha_i = \pi \rho_i$, the isotropic albedo for ith narrowband

$$= E_i / \cos\zeta$$

E_o = broadband scaled radiance $= \pi \int L_\lambda \, d\lambda \,/ \int S_\lambda \, d\lambda$

α_o = broadband isotropic albedo $= E_o / \cos\zeta$

$$A = \frac{1}{\pi H} \int_0^H \left\{ \int_0^{2\pi} \int_0^{\pi/2} \alpha_o \cos\theta \sin\theta \, d\theta \, d\phi \right\} dt = \alpha_o \chi f_t$$

where χ is the anisotropic correction factor (from angular dependancy model) and f_t is the diurnal correction factor (from directional model) for the instantaneous albedo $\alpha_o \chi$. Both χ and f_t are functions of the surface type. χ is the ratio of the true radiant exitance to the assumed isotropic exitance; f_t is the ratio of the daily average albedo to the instantaneous albedo.

The relationships that are determined empirically herein can be expressed in the following terms:

$$\alpha_o = a_o + \sum_{i=1}^{n} a_i \alpha_i \qquad (1)$$

and

$$E_o = b_o + \sum_{i=1}^{n} b_i E_i \qquad (2)$$

where n is determined by the number of spectral intervals, and the coefficients "a" and "b" are determined through multiple regression. These expressions, then define the instantaneous broadband isotropic albedo and scaled radiance from the narrowband terms. Although these broadband terms are the specific objective of the algorilthms derived, angular information should be carried along for subsequent applications of bidirectional and directional models. The narrowband data may also be used as a selection tool (through scene identification) for application of angular models to the broadband radiances.

3.0 Data

3.1 Model Simulation

For guidance, an initial narrowband-broadband feasibility simulation was performed with data from the extensive computations based on the Dave radiative transfer model (Dave, 1978). Spectral radiances cover the range 0.3 to 2.5 micrometers in 77 unequally spaced intervals. Models include options for up to three different scattering and absorbing aerosol distributions but only single fixed water vapor and ozone distributions. Results are obtainable for 7 solar zenith angles, 34 relative azimuth angles and up to 110 local zenith angles. Arbitrary spectrally-varying surface reflectances are easily introduced. Five major (typical) surface types were included in the simulations: (1) Ocean, (2) Vegetation, (3) Desert, (4) Cloud, and (5) Snow. All surfaces were treated as Lambertian in the broadband and AVHRR sensor simulations; ocean surface reflectances in specular directions are most affected by this assumption. The spectral resolution in the dataset permitted approximation of spectral response functions for simulation of the narrowband measurements. However, the simulated measurements were idealized in that surfaces were considered to be homogeneous (one type at a time) and isotropic. No shadows were considered, and no variations in atmospheric path were accounted for. Instrument noise was ignored; the principal means for obtaining a range of radiance magnitudes in the simulations for a given surface was by varing the solar zenith angle.

Figure 1 illustrates, for two solar angles, the spectral irradiance on a horizontal surface at the top of the atmosphere and on the earth's surface for a non-reflecting lower boundary. The atmospheric spectral albedo, or reflectance, is illustrated according to the scale on the right side. The difference between spectral irradiance curves represents atmospheric attenuation. The large peak in atmospheric reflection occurs in the UV portion of the spectrum. Spectral positions of the AVHRR Channels 1 (0.58-0.68 um) and 2 (0.72-1.10 um) are indicated in Figure 1. The illustrated spectral range encompasses the region covered by computations with the Dave model. Approximately one percent of incident energy remains at the shortwave tail below 0.3 and less than four percent in the longwave tail beyond 2.5 um. (The ERB broadband measurements extend spectrally to cover over 99 percent of incident energy). Using the entire illustrated spectral range to define the unfiltered broadband response, multivariate regressions were performed with the simulated broadband scaled radiance and the AVHRR narrowband scaled radiances, in accordance with Eq. (2). (Actual shortwave AVHRR measurements were calibrated and reported in terms of the scaled radiance used here.) By using the regression coefficient derived for channels 1 and 2, the broadband scaled radiances are estimated from the narrowband data and compared in Figure 2 with "true" broadband scaled radiances. With the exception of the brightest snow points in Figure 2, the simulated results suggest

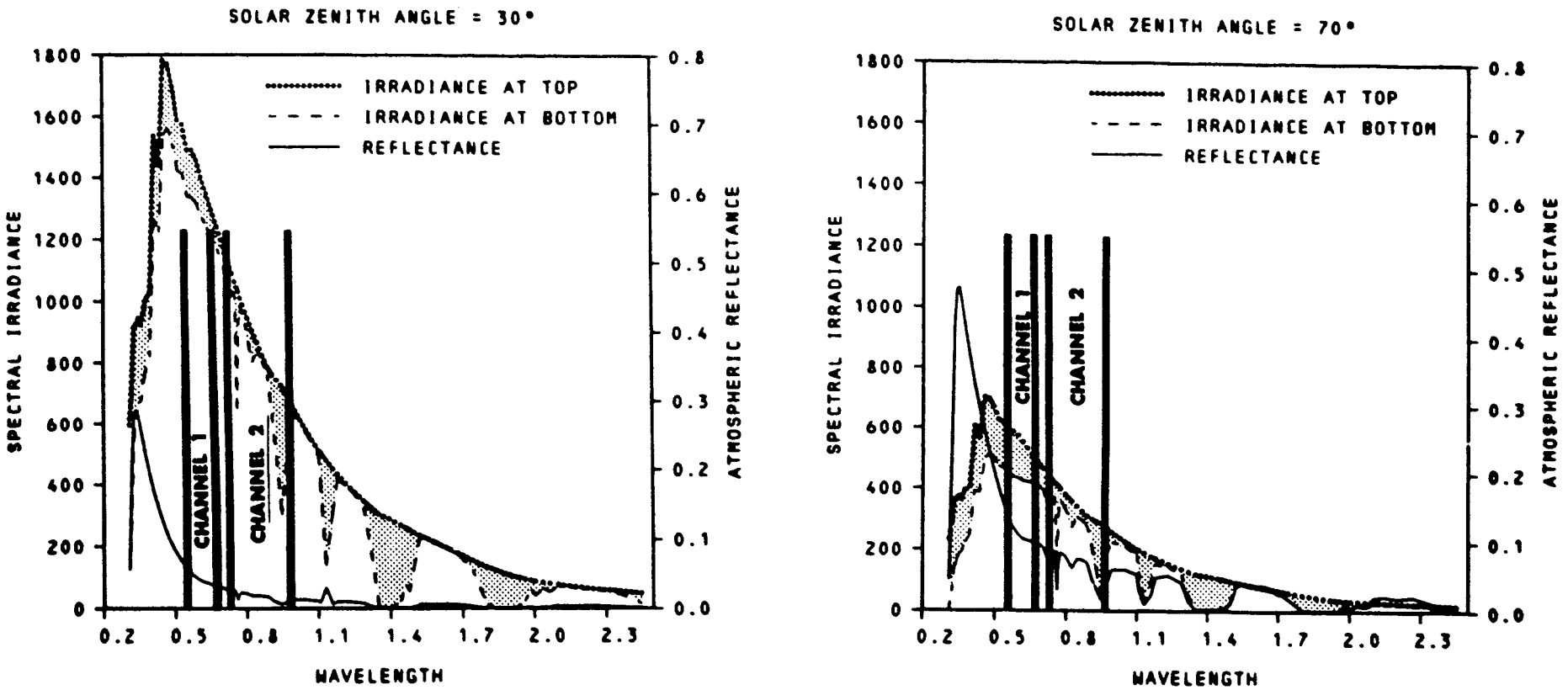

Figure 1. Solar Spectral Irradiance at the Top and Bottom of the Atmosphere, and the Atmospheric Reflectance for Solar Zenith Angles of 30 degrees and 70 degrees.

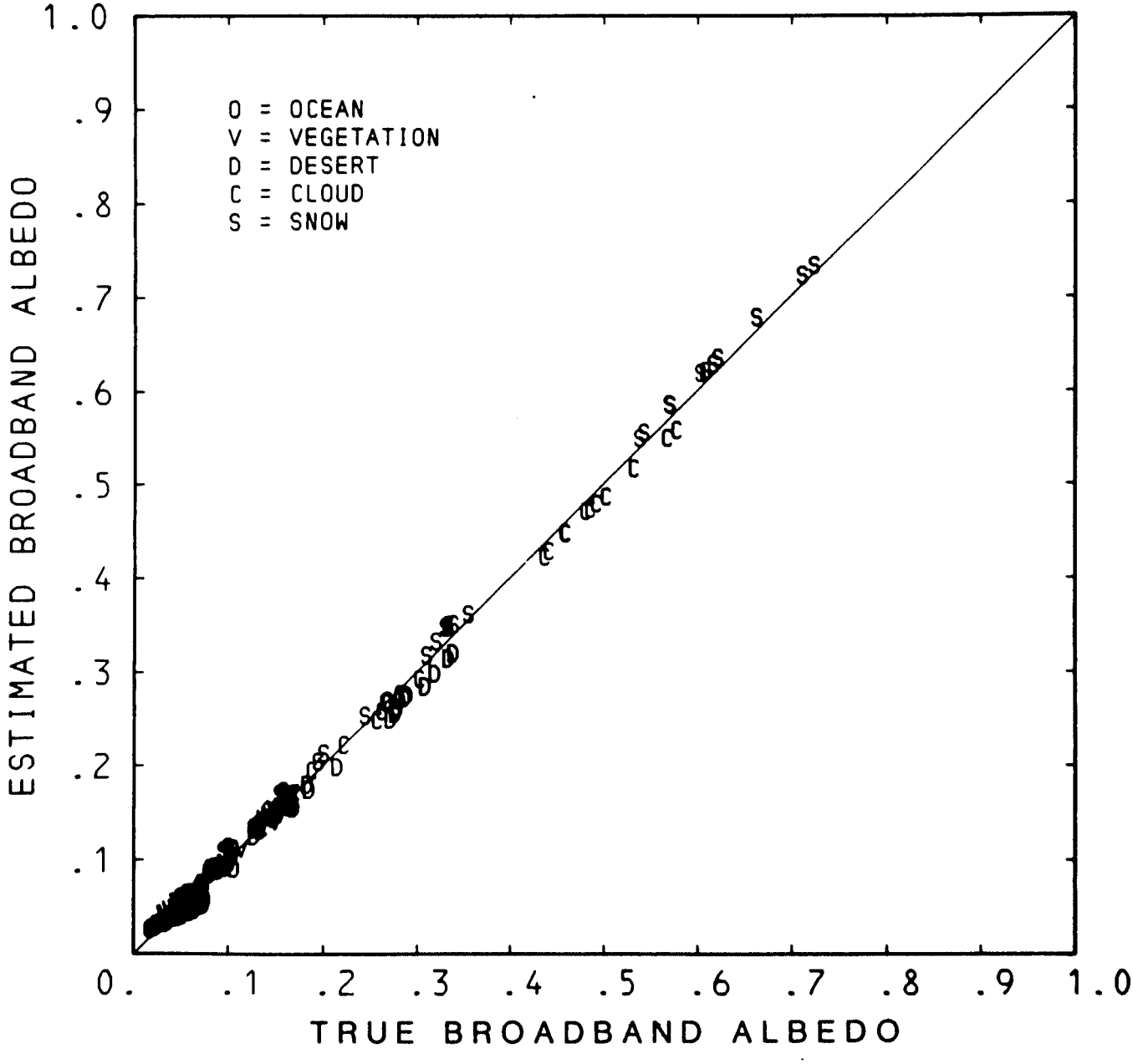

Figure 2. Comparison of Model Generated Albedo Values.

that a quasilinear relationship exists between the broadband scaled radiance estimated from narrowband measurements and the "true" broadband scaled radiance, regardless of surface type. The brightest snow points are unrealistic because of the small solar zenith angles associated with them. The acceptability of a linear relationship will depend on the scatter that arises with real data.

Table 1 summarizes some of the regression results for individual surfaces and for a combination of all surface types. Since NOAA's operational shortwave radiation budget products have been derived from AVHRR Channel 1 data, results for regressions using only Channel 1 to estimate broadband scaled radiances are included also. The main difficulty with Channel 1 alone is its failure to respond to the surface reflections associated with vegetation.

Table1 Coefficients from Regression Analyses of Simulated Broadband and AVHRR Narrowband Overhead-Sun Isotropic Albedos (Scaled Radiances)

	AVHRR Channels 1 and 2			AVHRR Channel 1	
	Intercept (%)	Ch. 1 Coeff.	Ch. 2 Coeff	Intercept (%)	Slope Ch. 1
Ocean	0.10	1.23	-0.34	0.79	0.91
Vegetation	0.69	0.49	0.44	1.33	1.27
Desert	0.34	1.20	-0.26	0.45	0.94
Cloud	0.66	0.63	0.21	0.78	0.80
Snow	0.47	0.40	0.43	0.83	0.76
COMBINATION	1.72	0.39	0.44	2.92	0.75

When both AVHRR Channel 1 and 2 are used in estimation

(simulated) of broadband scaled radiance, for the combination of all surface types, the relative weight of each channel is similar, but with a slightly larger coefficient for Channel 2. The greater spectral width of Channel 2 encompasses a greater portion of incident solar radiation, even though the higher surface reflections and generally lower atmospheric transmittance in Channel 1 leads to a greater outgoing spectral flux density.

3.2 Empirical Data

3.2.1 Broadband (ERB)

The broadband data were generated from the Nimbus-7 ERB narrow field-of-view (NFOV) shortwave scanning channels (Jacobowitz, et al., 1984). These channels have a spectral response ranging from 0.2 to 4.8 micrometers. An extensive ERB NFOV (shortwave and longwave) data set exists, including cloud information and surface type for geographical grid areas over the globe. Solar and satellite zenith angle information is included, along with relative azimuth increments (Stowe, and Fromm, 1984). Each grid area covers about (165 km)2 with zonal boundaries spaced 1.5 degrees of latitude. The ERB NFOV instrument functioned from November 1978 until June 1980.

3.2.2 Narrowband (AVHRR)

Narrowband data consisted of daylight portions of three adjacent NOAA-7 orbits. The orbits were chosen for the variety of surface types covered. AVHRR channels 1 and 2 Global Area Coverage (GAC) data used have a nadir resolution of 1.1 x 4.0 km. The GAC data are the same type of data used for NOAA radiation budget products. The GAC data consist of four out of five consecutive scan spots of every third scan line of the highly resolved Local Area Coverage (LAC) data (Gruber, et al, 1983). The individual GAC data spots were used for determination of scene types, and then averaged over larger views corresponding to an ERB measurement. For matchup with ERB, calculations were made of solar and satellite zenith angles and relative azimuth angles. Broadband longwave estimates also were made as a tool for screening to ensure proper cloud matchups. Inasmuch as the actual AVHRR data used were obtained from 1981 (not coincident with the broadband ERB data), matchups between AVHRR and ERB data required procedures that minimized differencs due to space and time variabilities. One procedure restricts data (over the same target types) to those with the same solar zenith angle and approximately the same satellite zenith angle, while nearly matching the relative azimuth angles, if possible, or assuming symmetry with respect to the principal plane of the sun. The

only difficulty with this approach is the time dependence of cloud surface and land surface albedos. The other procedure is to adjust the broadband data, through the application of bidirectional and directional angular models to achieve an angular matchup with the AVHRR data. The difficulties here are the requirement for careful scene identification and the uncertainty introduced by application of statistically determined models to specific point values. Results presented here demonstrate only the AVHRR data that are matched (angularly) with ERB broadband data, without adjustment of the latter.

4.0 Results (Empirical)

Broadband-narrowband relationships were examined empirically for individual surface types as well as for the combination of all surface types. Sample sizes for specific surface types were limited as a result of the extensive screening demanded to ensure matches of AVHRR and ERB data in terms of solar zenith, satellite zenith, and relative azimuth angles (despite the differences in satellite times). This limitation and the tendency for clustering of data from a given background led to less stable narrowband-broadband statistics for individual surfaces than for the overall combination of all data points. Nevertheless, datasets that were generated contained meaningful representations of the various surface types. Figure 3 is a comparison of AVHRR

Channel 1 and Channel 2 albedo. The data segregate naturally, with water surfaces, clouds, and snow showing higher Channel 1 reflectance while vegetation and, to a lesser extent, desert surfaces show higher Channel 2 reflectance. This conformity to expectations also serves as a partial assurance as to reasonableness of the relative calibration of the AVHRR channels.

Until now only a single channel (AVHRR Channel 1) has been used to estimate radiation budget parameters (Gruber, 1978). Figure 4 illustrates AVHRR Channel 1 data plotted against ERB broadband albedo for matched scenes; the AVHRR data points correspond to those in Figure 3. It is apparent that the vegetated areas and, to a lesser extent, the desert areas are somewhat underestimated by Channel 1, with some overestimation for other surfaces just as in the comparison with AVHRR Channel 2. Of course, the overall scatter of data points is larger in Figure 4, since none of the points are coincident views of the same targets as in Figure 3. Especially noticable is the larger scatter of the cloud points; this emphasizes the extreme difficulty in matching a cloud scene from independent views at different times.

From Figure 4, it would seem that inclusion of Channel 2 should improve the relationship to broadband albedos. Figure 5 illustrates, for the same matchup, the AVHRR Channel 2 data

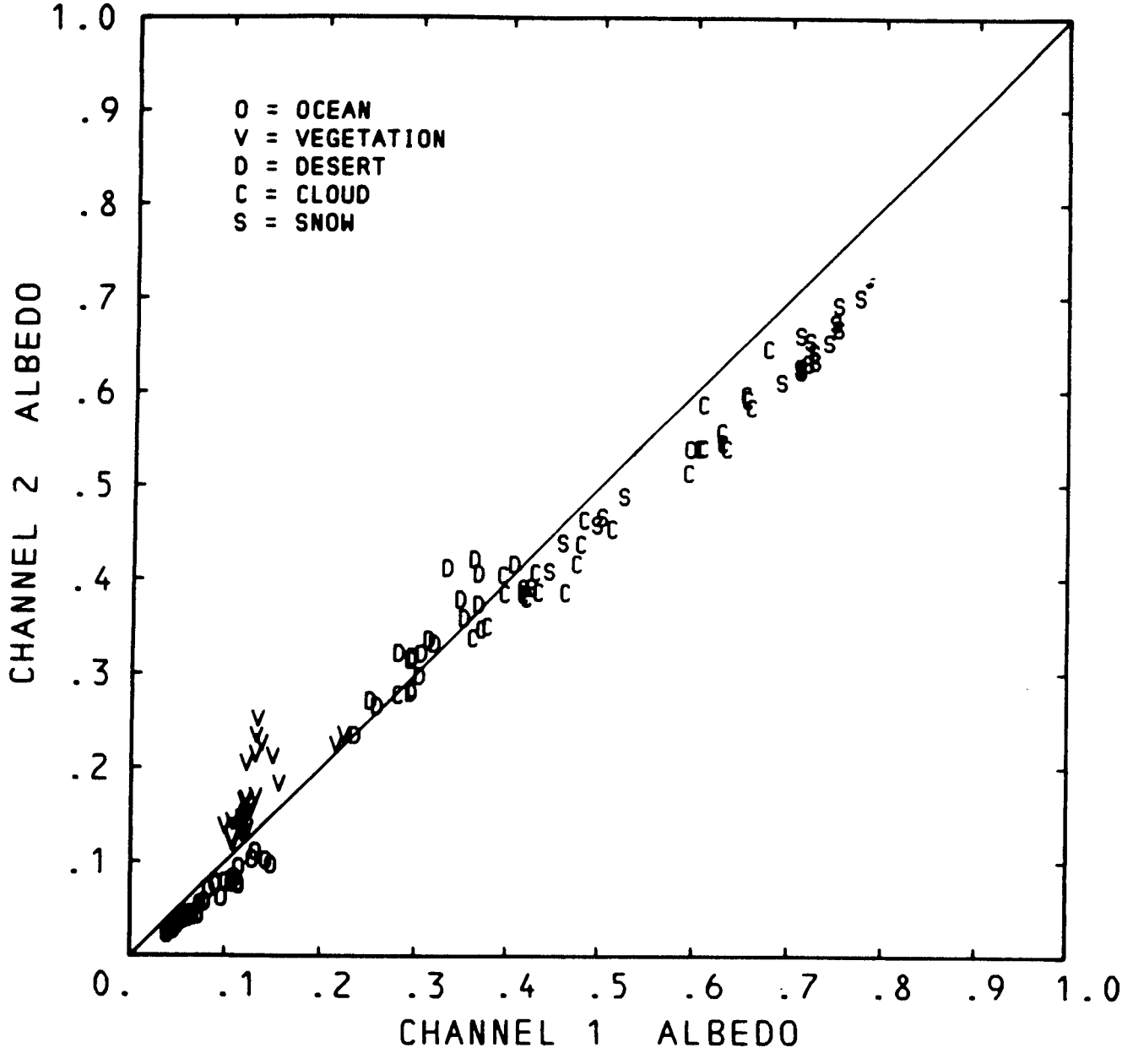

Figure 3. Comparison of AVHRR Narrowband Observations.

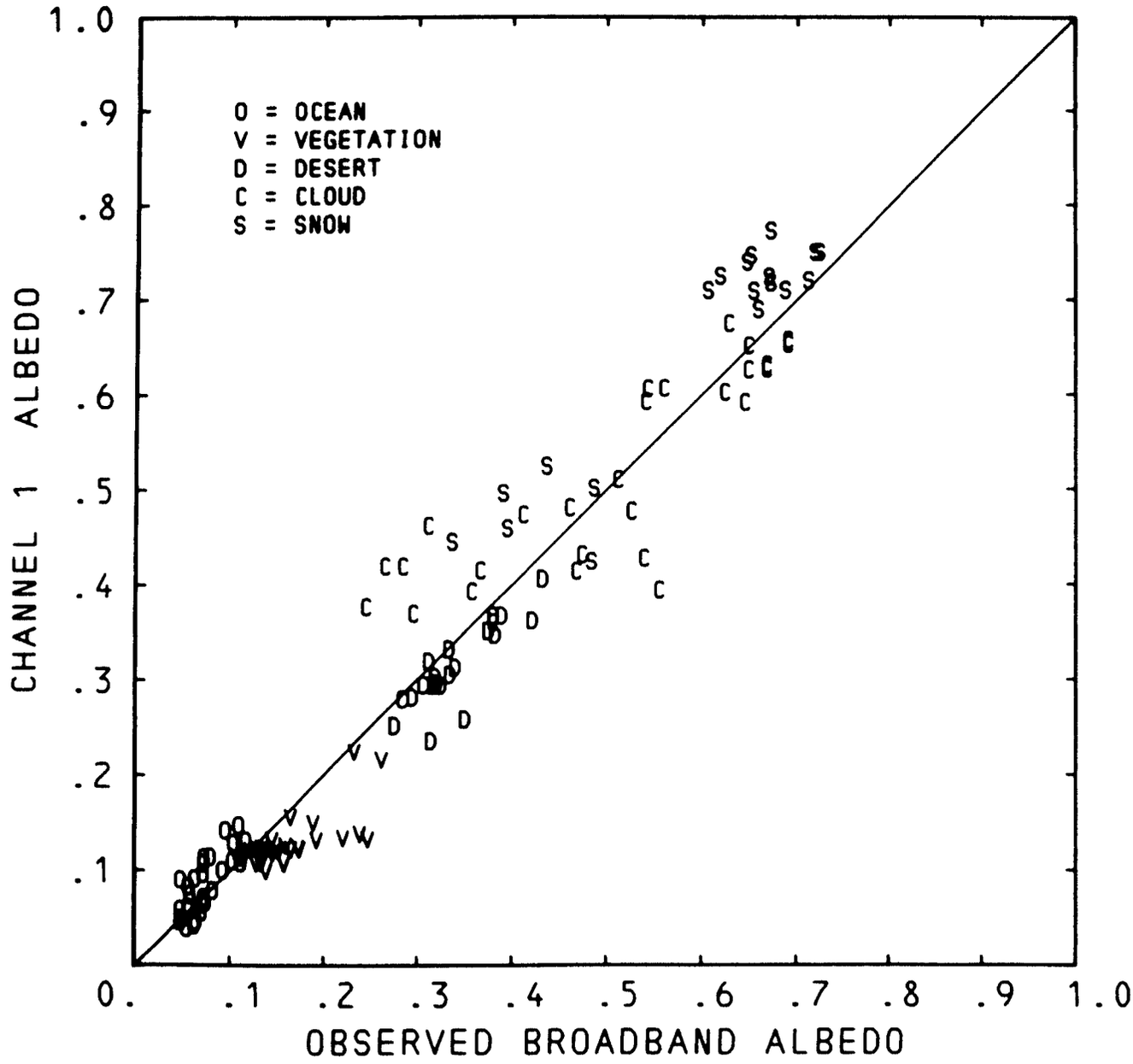

Figure 4. Comparison of AVHRR Channel 1 Narrowband Albedo with ERB Broadband Observations.

against the ERB broadband. Ocean albedos are somewhat underestimated by Channel 2, as are the brighter clouds. Vegetation albedos may be slightly overestimated. In general, the relationship of Channel 2 with ERB is similar to that with Channel 1 and ERB, except that better correspondence over vegetation is achieved.

Multivariate regressions were performed, linking the broadband ERB data to the AVHRR Channels 1 and 2, taken as independent variables in accordance with Eq. 1 and 2. Results of the regressions are summarized in Table 2. The coefficients derived from the regressions for the combination of all surface types were also applied to AVHRR observations to obtain the dependent broadband estimates directly from the AVHRR data. These broadband estimates were then compared with the observed ERB broadband data, as in Figure 6. It can be seen in Figure 6 that the linear regression relationship using both AVHRR channels leads to a successful depiction of broadband albedo over the entire range without bias for specific surfaces types. Of course, the largest scatter still occurs for cloud matchups; such scatter can only be reduced for coincident views.

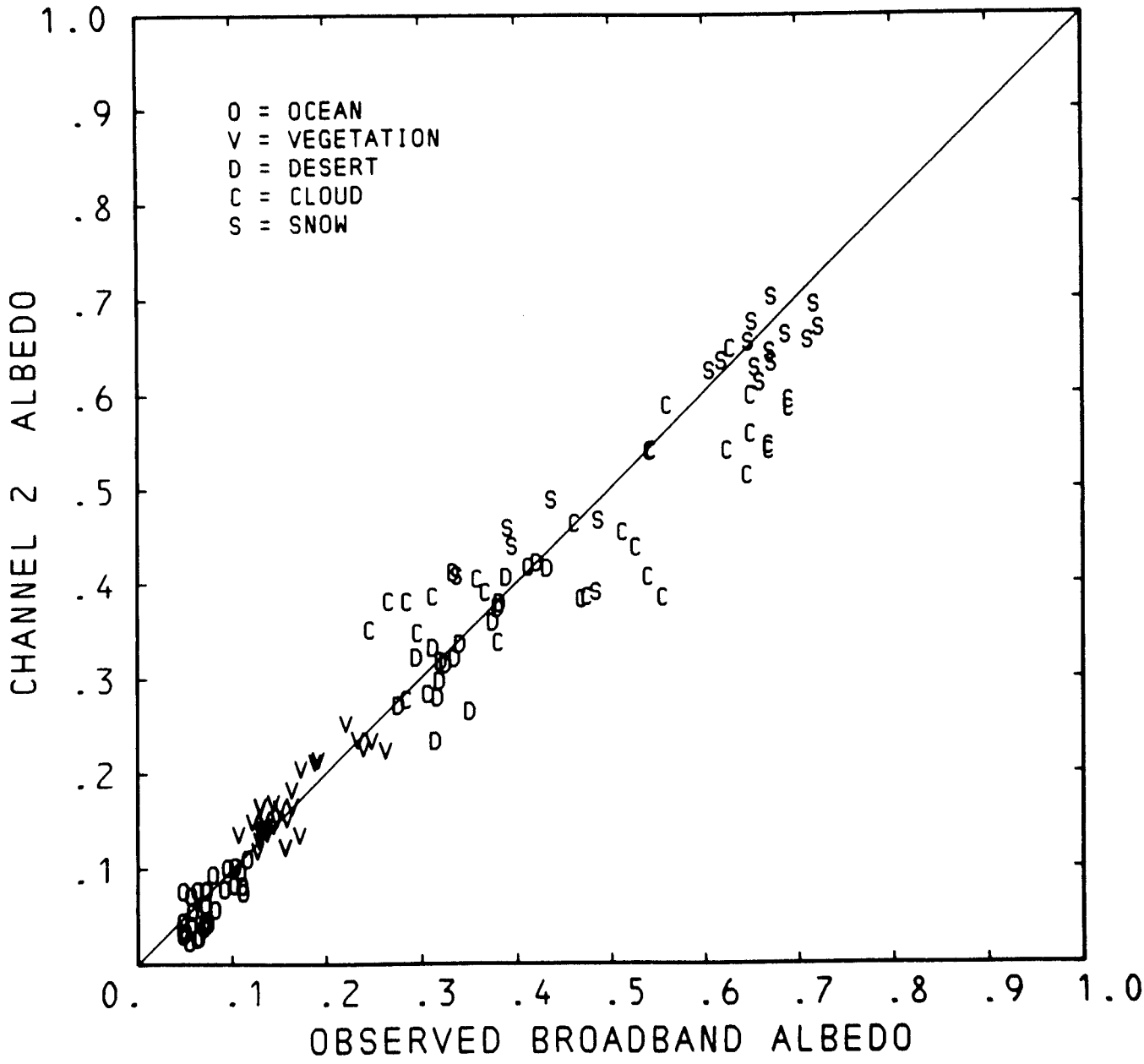

Figure 5. Comparison of AVHRR Channel 2 Narrowband Albedo with ERB Broadband Observations.

Table 2 Regression Statistics Derived from Angularly-Matched ERB Broadband and AVHRR Narrowband Bidirectional Reflectances

R2 = Explained Variance

RMSE = Root-Mean-Square-Error of Broadband Estimate

A_o = Intercept (%)

A_1 = AVHRR Ch. 1 Coeff.

A_2 = AVHRR Ch. 2 Coeff.

(#) = Standard Error of Estimate

SURFACE	R2	RMSE	A_o	A_1	A_2
		ISOTROPIC ALBEDO, CHANNELS 1 AND 2			
OCEAN	.638	1.365	2.585(0.763)	0.851(.318)	-0.392(.389)
VEGETATION	.754	2.126	-0.702(2.026)	0.361(.193)	0.732(.138)
DESERT	.715	2.422	9.321(4.176)	0.874(.329)	-0.070(.265)
CLOUD	.756	7.506	-6.219(6.591)	0.730(.648)	0.406(.756)
SNOW	.879	4.622	-5.125(6.973)	0.371(.772)	0.686(.915)
COMBINATION	.956	4.551	0.746(0.765)	0.347(.107)	0.650(.121)
		ISOTROPIC ALBEDO, CHANNEL 1			
OCEAN	.624	1.365	2.803(0.732)	0.540(.081)	
VEGETATION	.488	3.010	2.906(2.703)	1.040(.205)	
DESERT	.713	2.350	9.485(4.009)	0.794(.126)	
CLOUD	.753	7.410	-4.757(5.925)	1.072(.116)	
SNOW	.875	4.562	-2.223(5.723)	0.945(.087)	
COMBINATION	.945	5.041	2.466(0.769)	0.915(.020)	
		SCALED RADIANCE, CHS. 1 AND 2			
COMBINATION	.941	3.327	0.774(0.564)	0.326(.104)	0.663(.114)
		SCALED RADIANCE CH. 1			
COMBINATION	.924	3.744	1.826(.601)	0.917(.024)	

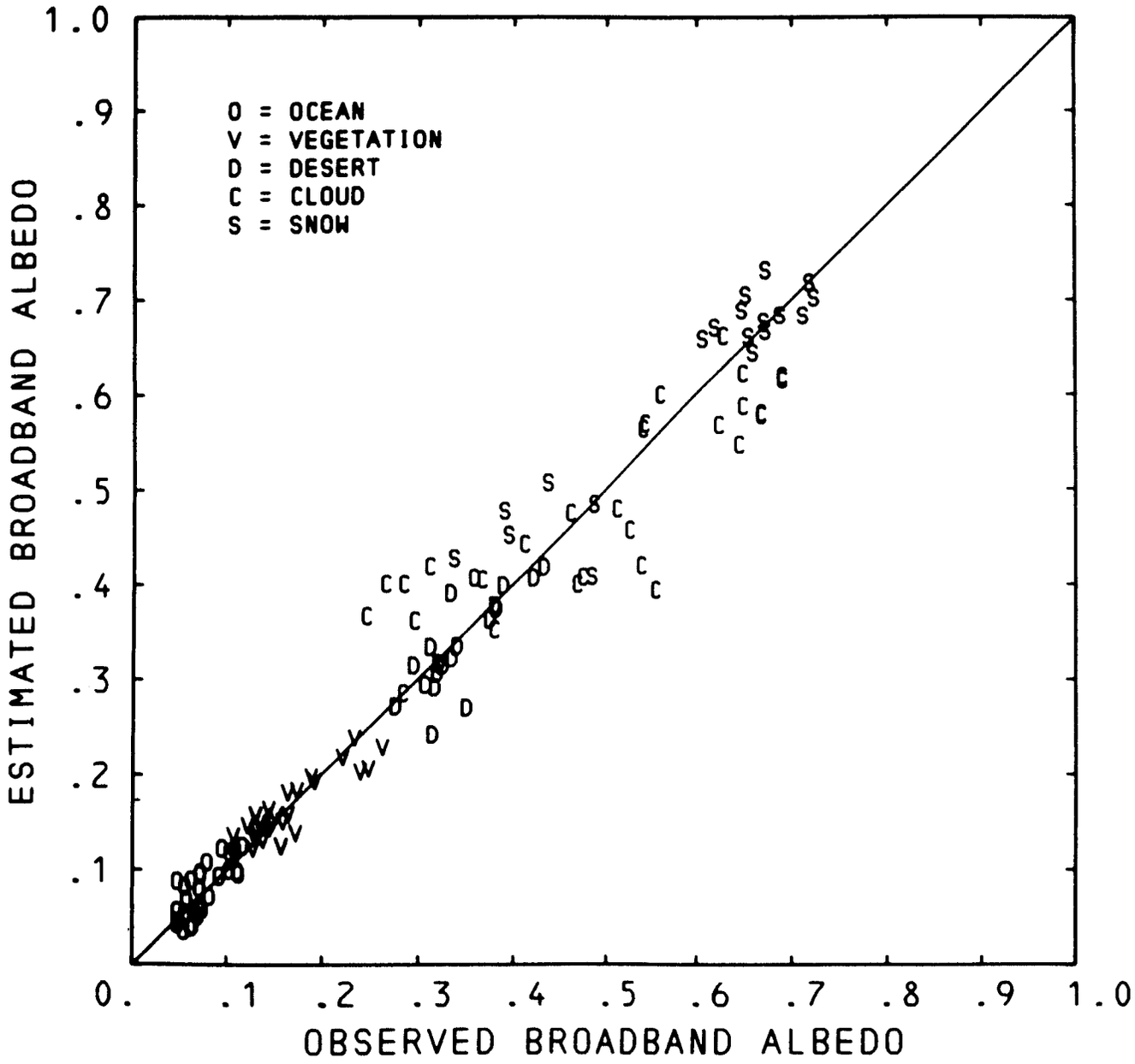

Figure 6. Comparison of Albedo Produced using a Linear Combination of AVHRR Channels 1 and 2 with ERB Broadband observations.

For comparison, broadband estimates also were obtained from an algorithm based solely on AVHRR Channel 1. These estimates are compared with the broadband ERB observations in Figure 7. Although the cloud-data scatter is similar in both Figures 6 and 7, it can be seen in Figure 7 that the single Channel 1 estimates tend to show overestimates for ocean and snow and underestimates for land surfaces, especially for vegetation. Thus, while the overall relationship between AVHRR Channel 1 broadband estimates and observations is similar to that for estimates based on both Channels 1 and 2, individual data points tend to be biased for different surface types.

The particular dataset used to generate coefficients appearing in Table 2 reveals the marked differences associated with the different surface types. The RMSE and offset (A_0) are indicated in percent. The large RMSE associated with clouds merely expresses the dissimilarities in the cloud backgrounds from independent scenes; for coincident views the RMSE would drop significantly. The explained variance (R^2) is higher for the pair of AVHRR channels than for Channel 1 alone, especially for vegetation. Practical emphasis of the narrowband-broadband relationship is on the combination of all surface types. As shown in Figure 6, a linear relationship is satisfactory and enables the broadband estimation of isotropic albedo or scaled radiance without scene identification. Furthermore, the explained variance is largest for the combination of all surface

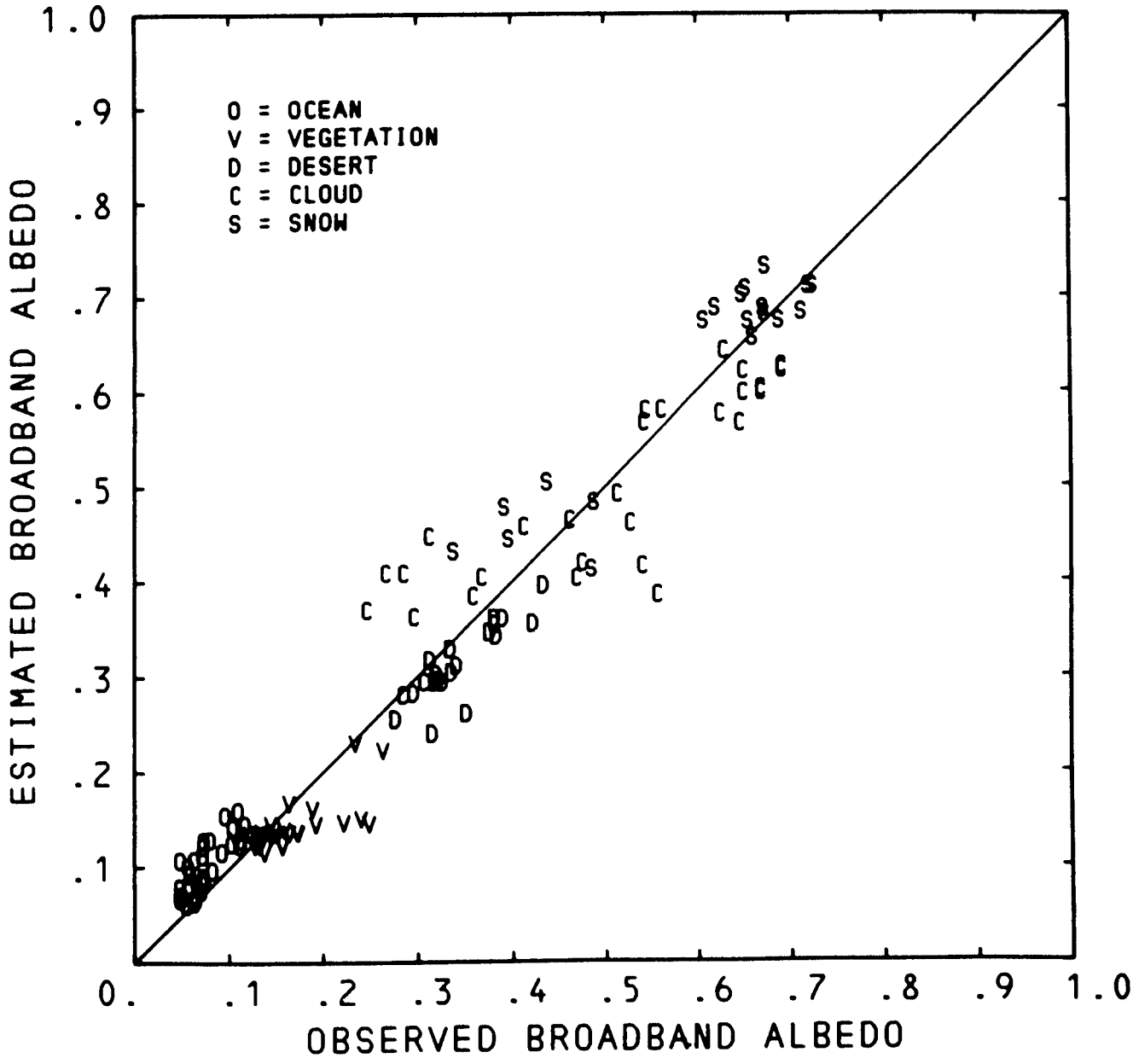

Figure 7. Comparison of Albedo Predicted by AVHRR Channel 1 Broadband Algorithm with ERB Broadband observations.

types, as a result of the much larger variance for the combination. Coefficients for the combination do not change significantly in going from isotropic albedo to scaled radiance. Additional studies of the sensitivity of the regression coefficients derived from empirical data have revealed or substantiated a number of factors, other than the obvious importance of measurement calibration. The coefficients are somewhat responsive to the makeup of the dataset, i.e., the representativeness of atmospheric and surface inhomogeneities and their mix. For some land surfaces the variations in anisotropy can be large, as it is for the ocean, so that a biased angular sampling of such surfaces could influence the regression relationship. On the whole, for angular matching of narrowband and broadband data there is a 95 percent probability that the coefficients for the combination will be within about 15 percent of their derived values. Furthermore, if one coefficient increased the other would decrease (a high negative correlation between the coefficients). The fact that the Channel 2 coefficient exceeds that for Channel 1 relates to the conclusion that Channel 2 accounts for more of the explained variance than Channel 1; uncertainty in Channel 2 as a result of signal variability is less than for Channel 1.

If instead of angular matching, angular models are applied to the broadband data to adjust the measurements to what would have been measured from the same angles encountered by the narrowband, then uncertainty is added. This uncertainty is

related to the statistical nature of the model as well as to model resolution and to the method of interpolation used in its application. However, the most troubling adjustment is for the solar zenith angle; it is better that the solar angles be matched so as to avoid adjustment.

Part of the difficulty with solar zenith angle occurs for very large zenith angles (low sun and long slant paths). Here, for example, the attenuation in the Chappius band of ozone can reduce the albedo of Channel 1 relative to that of Channel 2, and could lead to broadband albedo underestimates if only Channel 1 were used.

5.0 Conclusions

The broadband isotropic albedo (or the scaled radiance, which yields the isotropic albedo upon division by the cosine of the solar zenith angle) can be successfully estimated through a linear relationship to the narrow band isotropic albedos for AVHRR channels 1 and 2. Inclusion of channel 2 in the algorithm significantly improves the estimation of albedo over vegetated areas, while reducing the inherent single channele 1 overestimation of albedo for oceanic scenes. Furthermore, for the purpose of routinely generating and mapping radiation budget parameters, the linear relationship can be applied to matching angular conditions regardless of scene type. However, to

generate the true broadband shortwave flux density and albedo, and to determine daily averages, it is necessary to apply existing bidirectional reflectance and directional reflectance models to the estimated instantaneous isotropic albedos.

Much of the scatter in the approximated linear relationship arose from the inability to develop the relationship from coincident narrowband and broadband views. Inasmuch as the derived regression results were based on limited empirical data after extensive screening to obtain narrowband and broadband data for the same target types with the same solar zenith, satellite zenith, and relative azimuth angles, it is most urgent to extend the empirical testing of the relationship from coincident ERBE and AVHRR measurements from the NOAA-9 satellite. The AVHRR data may also be used for scene identification.

A specific uncertainty remaining with the broadband-narrowband isotropic albedo relationship is the possible angular dependencies, and especially the solar zenith angle, of the coefficients. It is recommended that the algorithm be expanded to include one or more functions of the pertinent angles in the regression as independent variables along with the narrowband albedos.

REFERENCES

Bowker, D.E., R.E. Davis, D.L. Myrick, K. Stacy and W.T. Jones, June 1985: Spectral Reflectances of Natural Targets for use in Remote Sensing Studies. NASA Ref. Pub., 1139.

Briegleb, B. and V. Ramanathan, 1982: Spectral and Diurnal Variations in Clear Sky Albedo. Journal of applied Meteorology, 21, 1160-1171.

Dave, S.V., 1978: Extensive Datasets of the Diffuse Radiation in Realistic Atmospheric Models with Aerosols and Common Absorbing Gases. Solar Energy, 21, 361-369.

Davis, P.A., E.R. Major, and H. Jacobowitz, 1984: An Assessment of Nimbus-7 ERB Shortwave Scanner Data by Correlative Analysis with Narrowband CZCS Data. J. Geophys. Res., 89, 5077-5088.

Gruber, A., I. Ruff, and C. Earnest, 1983: Determination of the Planetary Radiation Budget from TIROS-N Satellites. NOAA Technical Report NESDIS 3.

Gruber, A., 1978: Determination of the Earth - Atmosphere Radiation Budget From NOAA Satellite Data. NOAA Technical Report NESS 76.

Gruber, A., and J.S. Winston, 1978: Earth-atmosphere radiative heating based on NOAA scanning radiometer measurements. Bull. Amer. Meteor Soc., 59, 1570-1573.

Jacobowitz, H., HV. Soule, H.L. Kyle, F.B. House, and thee Nimbus-7 ERB Experiment Team, 1984: The Earth Radiation Budget (ERB) Experiment: An Overview. J. Geophys. Res., 89, 5021-5038.

Minnis, Patrick and Edwin F. Harrison, 1984: Diurnal Variability of Regional Cloud and Clear-Sky Radiative Parameters Derived from GOES Data. J. Climate and Applied Meteorology, Vol. 23, 993-1051.

Stowe, L.L., and M. Fromm, 1983: Nimbus-7 ERB Sub-target Radiance Tape (STRT) Data Base, NOAA Tech. memo NESDIS 3, National Oceanic and Atmospheric Administration, Washington, D.C.

Wiscombe, W.S. and S.G. Warren, 1980: A Model for the Spectral Albedo of Snow. I: Pure Snow. J. Atmos. Sci. 37 2734-2745.

Wydick, J.E., and P.A. Davis, 1983: Broadband albedo estimates from narrowband multispectral satellite measurements. Fifth conference on atmospheric radiation: Preprints, 403-406.

(Continued from inside cover)

NESDIS 6 Spatial and Temporal Distribution of Northern Hemisphere Snow Cover. Burt J. Morse (NESDIS) and Chester F. Ropelewski, October 1983. (PB84 118348)

NESDIS 7 Fire Detection Using the NOAA--Series Satellites. Michael Matson and Stanley R. Schneider (NESDIS), Billie Aldridge and Barry Satchwell (NWS), January 1984. (PB84 176890)

NESDIS 8 Monitoring of Long Waves in the Eastern Equatorial Pacific 1981-83 Using Satellite Multi-Channel Sea Surface Temperature Charts. Richard Legeckis and William Pichel, April 1984. (PB84 190487)

NESDIS 9 The NESDIS-SEL Lear Aircraft Instruments and Data Recording System. Gilbert R. Smith, Kenneth O. Hayes, John S. Knoll, and Robert S. Koyanagi, June 1984. (PB84 219674)

NESDIS 10 Atlas of Reflectance Patterns for Uniform Earth and Cloud Surfaces (NIMBUS-7 ERB--61 Days). V.R. Taylor and L.L. Stowe. (PB85 12440)

NESDIS 11 Tropical Cyclone Intensity Analysis Using Satellite Data. Vernon F. Dvorak, September 1984. (PB85 112951)

NESDIS 12 Utilization of the Polar Platform of NASA's Space Station Program for Operational Earth Observations. John H. McElroy and Stanley R. Schneider, September 1984. (PB85 1525027AS)

NESDIS 13 Summary and Analyses of the NOAA N-ROSS/ERS-1 Environmental Data Development Activity. John W. Sherman III, February 1984. (PB85 222743/43)

NESDIS 14 NOAA N-ROSS/ERS-1 Environmental Data Development (NNEEDD) Activity. John W. Sherman III, February 1985. (PB86 139284 A/S)

NESDIS 15 NOAA N-ROSS/ERS-1 Environmental Data Development (NNEEDD) Products and Services. Franklin E. Kniskern, February 1985. (PB86 213527/AS)

NESDIS 16 Temporal and Spatial Analyses of Civil Marine Satellite Requirements. Nancy J. Hooper and John W. Sherman III, February 1985. (PB86 212123/AS)

NESDIS 17 reserved

NESDIS 18 Earth Observations and The Polar Platform. John H. McElroy and Stanley R. Schneider, January 1985. (PB85 177624/AS)

NESDIS 19 The Space Station Polar Platform: Integrating Research and Operational Missions. John H. McElroy and Stanley R. Schneider, January 1985. (PB85 195279/AS)

NESDIS 20 An Atlas of High Altitude Aircraft Measured Radiance of White Sands, New Mexico, in the 450-1050 nm Band. Gilbert R. Smith, Robert H. Levin and John S. Knoll, April 1985. (PB85 204501/AS)

NESDIS 21 High Altitude Measured Radiance of White Sands, New Mexico, in the 400-2000 nm Band Using a Filter Wedge Spectrometer. Gilbert R. Smith and Robert H. Levin, April 1985. (PB85 206084/AS)

NESDIS 22 The Space Station Polar Platform: NOAA Systems Considerations and Requirements. John H. McElroy and Stanley R. Schneider, June 1985. (PB86109246/AS)

NESDIS 23 The Use of TOMS Data in Evaluating and Improving the Total Ozone from TOVS Measurements. James H. Lienesch and Prabhat K.K. Pandey, July 1985. (PB86108412/AS)

NESDIS 24 Satellite-Derived Moisture Profiles. Andrew Timchalk, April 1986. (PB86 232923/AS)

NESDIS 25 reserved

NESDIS 26 Monthly and Seasonal Mean Outgoing Longwave Radiation and Anomalies. Arnold Gruber, Marylin Varnadore, Phillip A. Arkin, and Jay S. Winston, October 1987. (PB87160545/AS)

NESDIS 27 Estimation of Broadband Planetary Albedo from Operational Narrowband Satellite Measurements. James Wydick, in press.

NESDIS 28 The AVHRR/HIRS Operational Method for Satellite Based Sea Surface Temperature Determination. Charles Walton, in press.

NESDIS 29 The Complementary Roles of Microwave and Infrared Instruments in Atmospheric Sounding. Larry McMillin, in press.

NOAA SCIENTIFIC AND TECHNICAL PUBLICATIONS

The National Oceanic and Atmospheric Administration was established as part of the Depar Commerce on October 3, 1970. The mission responsibilities of NOAA are to assess the socioeconomi of natural and technological changes in the environment and to monitor and predict the state of Earth, the oceans and their living resources, the atmosphere, and the space environment of the E

The major components of NOAA regularly produce various types of scientific and technical tion in the following kinds of publications:

PROFESSIONAL PAPERS—Important definitive research results, major techniques, and special investigations.

CONTRACT AND GRANT REPORTS—Reports prepared by contractors or grantees under NOAA sponsorship.

ATLAS—Presentation of analyzed data generally in the form of maps showing distribution of rainfall, chemical and physical conditions of oceans and atmosphere, distribution of fishes and marine mammals, ionospheric conditions, etc.

TECHNICAL SERVICE PUBLICATIO ports containing data, observations, instructions, etc. A partial listing includes data serials; prediction and outlook periodicals; technical manuals, training papers, planning reports, and information serials; and miscellaneous technical publications.

TECHNICAL REPORTS—Journal quality with extensive details, mathematical developments, or data listings.

TECHNICAL MEMORANDUMS—Reports of preliminary, partial, or negative research or technology results, interim instructions, and the like.

NATIONAL ENVIRONMENTAL SATELLITE, DATA, AND INFORMATION SERVICE
NATIONAL OCEANIC AND ATMOSPHERIC ADMINISTRATION
U.S. DEPARTMENT OF COMMERCE
Washington, D.C. 20233